

Observation of Asteroidal Occultation with Frame-integrating Video System

Toshihiro HORAGUCHI

Department of Science and Engineering, National Museum of Nature and Science,
4-1-1 Amakubo, Tsukuba, Ibaraki 305-0005, Japan
e-mail: horaguti@kahaku.go.jp

Abstract For the observation of asteroidal occultation, GPS time-inserted video system has been used at the observatory of Tsukuba since 2012. In order to target fainter stars, a new video camera that can integrate video frames was installed in 2019, and it makes opportunity of observation significantly increase such that the limiting magnitude has fallen to 15th magnitude from 12th magnitude. This paper reports the camera, observations, and the results of analysis, which tell us the sizes and the shapes of asteroids.

Key words: occultation, asteroid, video observation

1. Introduction

In the observation of asteroidal occultation, the use of video camera has attracted attention due to its high time-resolution. Asteroidal occultation is the phenomenon that occurs when an asteroid passes over a fixed star. During an asteroidal occultation, the shadow of the asteroid passes across the surface of the Earth, and the observers see the fixed star disappear for a short period of time. Observing the disappearance and reappearance times provides information on the size of the asteroid, and the shape can be traced out in case simultaneous observations of high time accuracy succeed at different locations. An occultation observation also brings precise position of the asteroid, and contributes to the refinement of the orbital elements and to the study of non-gravitational orbital transition, for example.

The author has been observing asteroidal occultation since 2012 at Tsukuba, where all of the research departments of National Museum of Nature and Science (NMNS) exist. The GPS time-inserted video observation system and the observations until 2018 are reported in the previous paper (Paper I)¹⁾. The output of the camera module is NTSC video signal, and its time resolution is 1/30 second. After the first camera, the author introduced a second-generation camera that

can integrate video frames aiming at fainter stars, and began observation in 2019.

In this paper, the author presents observations made with the new camera, which significantly increases the opportunities of detecting faint phenomena, and shows the results of timing analysis of characteristic observations in the past 5.5 years.

2. Observation

2.1 Frame-integrating Video Observation System

At Tsukuba branch, there is a 50 cm reflecting telescope whose focal length is 6 meters (F/12) as described in Paper I. The latitude and the longitude of the observatory is 36:06:05.8 North, 140:06:40.6 East at the geodetic system JGD2011, and the altitude is 40 meters above sea level. CCD video camera module is attached to the Cassegrain focus with $\times 1/2$ focal reducer, and the information of GSP time is added to each video frame by the time inserter, GHS-OSD, which is developed by Tsutomu Hayamizu and his colleagues^{2,3)}, as shown in Figure 1 of Paper I. The NTSC video signal is recorded onto VHS tape and has also been recorded simultaneously into PC SSD via A/D video convertor since May 2023.

The new camera module that has started observation in 2019 is Watec WAT-910HX of 1/2 inch monochromatic image sensor, while it was Watec WAT-

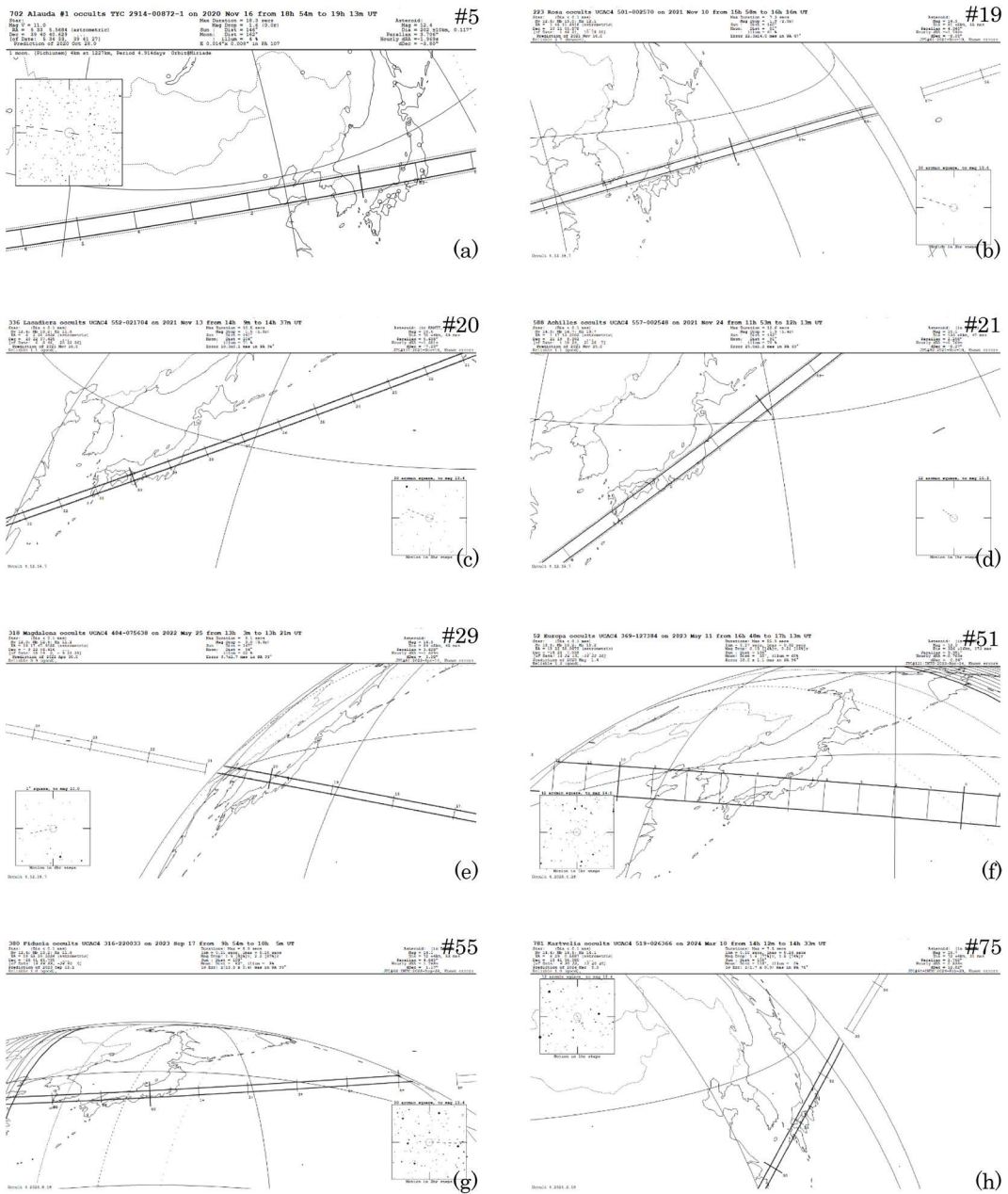


Fig. 1. Maps of predicted path of asteroidal occultation. The number at the upper right of each figure is the occultation number of Table 1, i.e., Fig. 1a is of occultation #5 by the asteroid (702)Alauda, for example. These are calculated and drawn by Occult software³⁾. The paths of asteroid's shadow projected by the occulted star on the surface of the Earth draw strips whose width corresponds to the projected size of each asteroid. The inset squares are star charts showing how the asteroid will approach the occulted star.

100N until 2018. Although such an ordinary camera as WAT-100N records video frame every 1/30 seconds, WAT-910HX can extend the exposure time in order to get image of fainter object. A video frame is composed

of two interlaced fields of odd lines and even lines. WAT-910HX is able to integrate those video fields optionally as $\times 2$, $\times 4$, $\times 8$, $\times 16$, $\dots \times 256$, though the time resolution of image is reduced.

Table 1. (Continued)

Occult. No.	Time (UT)		Asteroid			Target star			Max. t (sec)	
			Name	Mag.	D (km)	Name	R. A.	Dec.		Mag.
61	2023-11-21	16:17	(987)Wallia	14.6	49	UCAC4 622-030638	06:08:37.8	+34:12:57	14.2	4.9
62	2023-11-23	17:31	2004 VM131	24.0	87	UCAC4 513-024267	06:21:58.5	+12:27:45	13.6	4.2
63	2023-11-24	16:48	(535025)2014 WT509	22.9	120	UCAC4 504-009995	05:05:26.8	+10:42:23	13.0	5.0
64	2023-11-27	13:50	(1794)Finsen	16.1	38	UCAC4 496-023167	06:16:12.3	+09:01:13	13.0	3.1
65	2023-11-30	13:28	(882)Swetlana	13.9	44	UCAC4 557-006301	03:12:11.1	+21:12:39	12.8	5.6
66	2023-12-17	15:21	(4460)Bihoro	15.4	41	UCAC4 741-042739	06:07:02.8	+58:11:05	13.7	3.0
67	2023-12-23	13:15	(463)Lola	15.2	20	UCAC4 661-051337	07:46:15.8	+42:09:12	13.7	1.9
68	2023-12-23	14:13	(1385)Gelria	14.6	20	UCAC4 549-033995	06:51:25.8	+19:45:19	15.4	1.7
69	2023-12-23	15:44	(85807)1998 WR10	18.9	22	UCAC4 424-037041	07:33:19.1	-05:13:34	14.2	1.4
70	2024-01-13	12:40	(1583)Antilochus	15.8	107	UCAC4 366-047846	08:35:42.9	-16:57:21	13.5	6.8
71	2024-01-16	15:19	(210)Isabella	13.3	76	UCAC4 593-013224	04:36:49.2	+28:34:28	12.6	30.3
72	2024-02-16	09:36	(9829)Murillo	17.6	26	UCAC4 526-049109	08:49:32.1	+15:02:05	13.4	2.0
73	2024-03-09	15:49	(26375)1999 DE9	21.2	461	GaiaDR3 3526256287040798848	12:54:42.8	-12:41:23	13.0	21.5
74	2024-03-10	12:56	(1832)Mrkos	16.3	29	UCAC4 420-053200	10:34:20.1	-06:04:51	13.3	1.9
75	2024-03-10	14:31	(781)Kartvelia	15.7	72	UCAC4 519-026366	06:29:00.6	+13:41:36	14.4	7.5
76	2024-05-14	10:50	(92)Undina	13.3	121	UCAC4 577-039927	07:37:16.9	+25:21:38	14.2	4.0

* Column (1): serial number of occultation, (2): event time of occultation around Japan, (3–5): name, magnitude, and diameter estimated from previous observations of occulting asteroid, (6–9): name, right ascension, declination, magnitude of occulted star, (10): predicted duration of occultation at maximum.

2.2 Prediction of Asteroidal Occultation and the Observation

Asteroidal occultations are observed all over the world, and the predictions are provided from various observer groups such as International Occultation Timing Association (IOTA)⁴⁾. Occult is a useful software that is developed by a member of IOTA, David Herald⁵⁾, and used by many observers in the world for prediction, observation report, etc. IOTA/EA, which is established last year with the aim of promoting occultation research in East Asia, presents notable occultations that can be observed in East Asia region in its Web site^{6,7)}. Fig. 1 is the examples of prediction, which are calculated and drawn by Occult software and show the paths of asteroid's shadow projected by the occulted star on the surface of the Earth.

Table 1 is the list of asteroidal occultations observed by the author since 2019 using the new frame-integrating camera. There were 254 occultations planned to be observed, but accomplished were 76 occultations (30%) due to weather condition. While the limiting magnitude of occulted star observable by WAT-100N was about 12th magnitude, WAT-910HX can observe occultations nearly 15th magnitude as you can see in Table 1. The function of frame integration improves the S/N ratio of image, and enables observation of fainter star, of less magnitude drop, at near horizon, and in hazier sky. As a result, the number of successful

observation remarkably increases from 4 times/year to 14 times/year, and as for the detection of magnitude drop, 0.4 times/year to 7 times/year.

3. Analysis of Video Observations and the Results

The analysis of video images was done by the software Limovie^{8,9)}, as same as Paper I. Limovie is developed by Kazuhisa Miyashita who is a member of IOTA/EA, and measures the brightness of a star in each video frame automatically with the function that traces the position of a star fluctuating due to atmospheric scintillation, etc. Limovie provides two methods of brightness measurement, aperture photometry and PSF (Point Spread Function) photometry, and the author selects the method depending on the image quality that has relation to sky condition.

Fig. 2 is the examples of light curve, each of which shows not only the brightness measurement of Limovie but also the result of fitting to determine the time of disappearance and reappearance respectively. Table 2 is the result of occultation times and durations measured from the light curves as shown in Fig. 2. A duration time only provides a length of chord along the direction of asteroid movement, but the information of its shape can be obtained in case many observations of high time accuracy at different locations are compiled. Fig. 3 is the examples of compiled result,

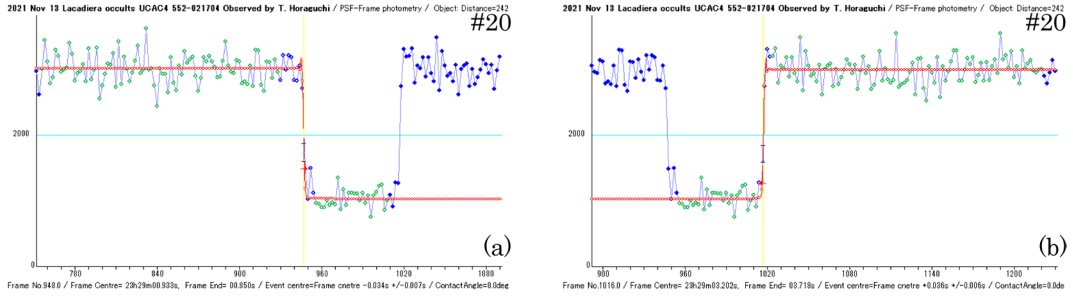


Fig. 2. Light curves of the occultation #20 by the asteroid (336)Lacadiera. The horizontal axes are video frame number, and the vertical axes are brightness. The respective red line shows the result of fitting to determine the time of (a) disappearance and (b) reappearance by Limovie^(8,9).

Table 2. Result of occultation times and durations

occult. No.	Asteroid	Occultation time (UT)	Duration (sec)
4	(451)Patientia (1st drop)	2020-05-02 13:49:57.664 ± 0.017 - 13:50:27.847 ± 0.017	30.18
4	(451)Patientia (2nd drop)	2020-05-02 13:50:09.759 ± 0.017 - 13:50:17.900 ± 0.017	8.14
5	(702)Alauda	2020-11-16 18:58:54.146 ± 0.017 - 18:59:08.577 ± 0.017	14.43
6	(788)Hohensteina	2020-12-04 09:14:05.6 ± 0.3 - 09:14:08.9 ± 0.3	3.3
10	(156)Xanthippe	2021-01-02 19:03:31.75 ± 0.10 - 19:03:37.24 ± 0.11	5.5
12	(150)Nuwa	2021-01-19 13:26:51.97 ± 0.02 - 13:27:00.49 ± 0.04	8.52
14	(740)Cantabria	2021-07-19 13:52:12.81 ± 0.05 - 13:52:15.79 ± 0.04	2.98
19	(223)Rosa	2021-11-10 16:00:36.148 ± 0.006 - 16:00:36.818 ± 0.005	0.67
20	(336)Lacadiera	2021-11-13 14:29:00.847 ± 0.006 - 14:29:03.182 ± 0.005	2.34
21	(588)Achilles	2021-11-24 12:01:17.57 ± 0.02 - 12:01:24.72 ± 0.03	7.15
23	(410)Chloris	2021-12-22 17:37:58.64 ± 0.03 - 17:38:05.20 ± 0.04	6.56
24	(426)Hippo	2021-12-27 13:54:45.692 ± 0.002 - 13:54:54.742 ± 0.002	9.050
25	(462)Eriphyla	2022-01-02 09:09:33.58 ± 0.10 - 09:09:34.35 ± 0.05	0.77
26	(737)Arequipa	2022-02-02 10:47:20.69 ± 0.05 - 10:47:23.34 ± 0.07	2.65
27	(1351)Uzbekistaniya	2022-02-05 12:10:37.96 ± 0.04 - 12:10:42.55 ± 0.05	4.59
28	(2008)Konstitutsiya	2022-03-07 11:27:24.1 ± 0.3 - 11:27:27.45 ± 0.13	3.3
29	(318)Magdalena	2022-05-25 13:19:38.154 ± 0.012 - 13:19:41.566 ± 0.010	3.412
38	(539)Pamina	2022-09-06 11:29:21.995 ± 0.002 - 11:29:29.359 ± 0.003	7.364
39	(227)Philosophia	2022-10-04 12:59:56.75 ± 0.05 - 13:00:02.06 ± 0.04	5.30
40	(1285)Julietta	2022-10-19 13:11:48.731 ± 0.006 - 13:12:03.535 ± 0.006	14.804
45	(259)Aletheia	2023-01-12 17:08:36.80 ± 0.07 - 17:08:50.03 ± 0.05	13.23
47	(25)Phocaea	2023-02-15 12:56:44.450 ± 0.012 - 12:56:48.328 ± 0.010	3.878
48	(3876)Quaide	2023-03-08 09:34:14.337 ± 0.003 - 09:34:19.800 ± 0.004	5.463
49	(586)Thekla	2023-04-09 12:08:21.795 ± 0.006 - 12:08:30.545 ± 0.006	8.750
50	(191)Kolga	2023-05-03 12:24:18.21 ± 0.04 - 12:24:19.95 ± 0.06	1.74
52	(1142)Aetolia	2023-08-18 12:53:03.253 ± 0.003 - 12:53:04.090 ± 0.004	0.837
54	(203)Pompeja	2023-09-12 09:56:37.25 ± 0.13 - (cloudy)	—
55	(380)Fiducia	2023-09-17 10:00:28.488 ± 0.004 - 10:00:30.982 ± 0.005	2.494
57	(154)Bertha	2023-11-05 12:14:41.51 ± 0.13 - 12:14:49.73 ± 0.13	8.22
58	(154)Bertha	2023-11-07 16:45:58.795 ± 0.015 - 16:46:01.378 ± 0.015	2.58
59	(35)Leukothea	2023-11-09 10:46:48.8 ± 0.3 - 10:46:54.9 ± 0.3	6.1
61	(987)Wallia	2023-11-21 16:17:47.95 ± 0.02 - 16:17:48.88 ± 0.03	0.93
65	(882)Swetlana	2023-11-30 13:28:30.727 ± 0.009 - 13:28:36.168 ± 0.009	5.441
66	(4460)Bihoro	2023-12-17 15:21:08.141 ± 0.007 - 15:21:08.687 ± 0.006	0.546
67	(463)Lola	2023-12-23 13:15:50.98 ± 0.02 - 13:15:52.19 ± 0.02	1.21
70	(1583)Antilochus	2024-01-13 12:40:34.36 ± 0.13 - 12:40:41.12 ± 0.14	6.76
71	(210)Isabella	2024-01-16 15:19:12.11 ± 0.04 - 15:19:14.30 ± 0.02	2.19
75	(781)Kartvelia	2024-03-10 14:31:38.17 ± 0.03 - 14:31:40.26 ± 0.06	2.09
76	(92)Undina	2024-05-14 10:50:13.76 ± 0.11 - 10:50:17.83 ± 0.11	4.07

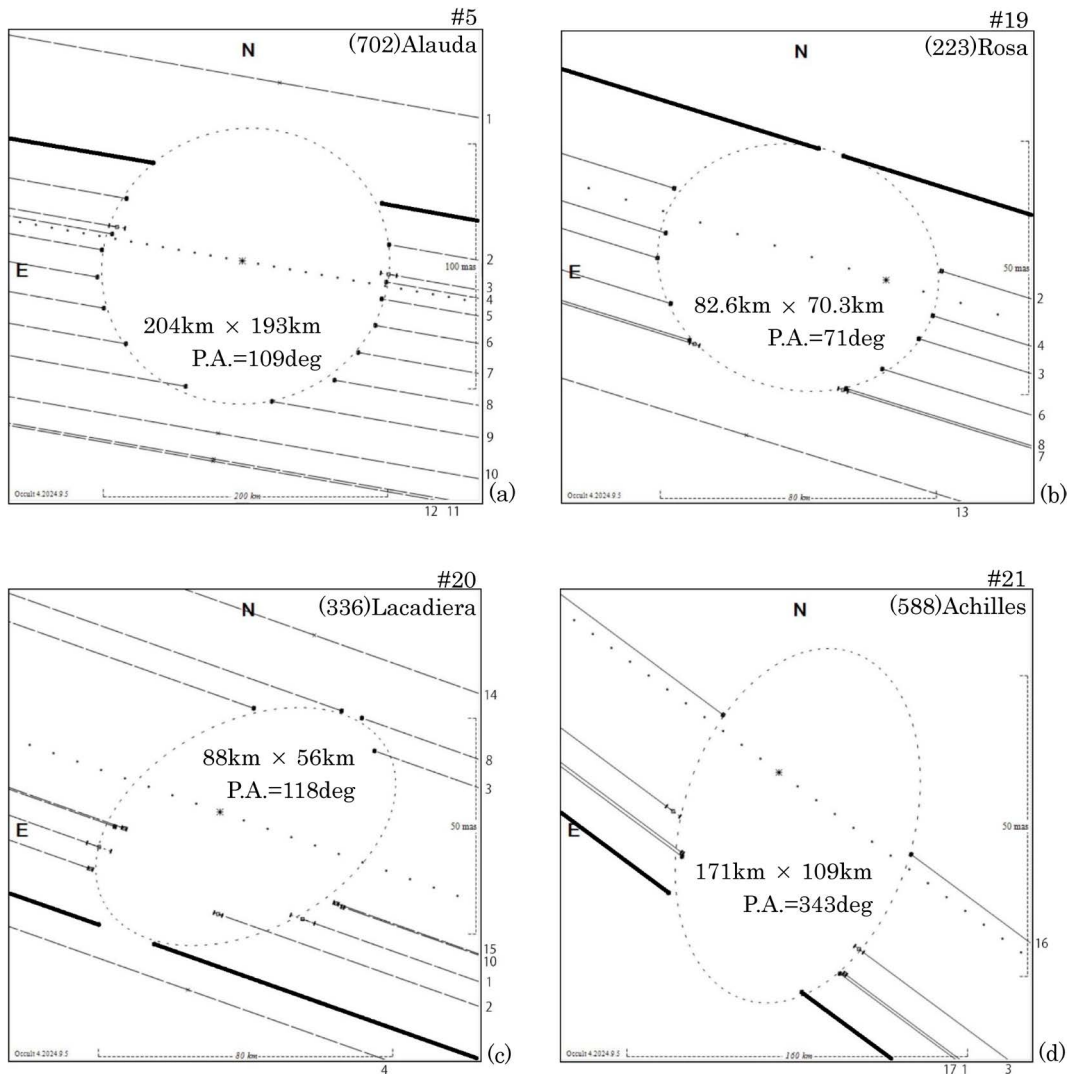


Fig. 3. Results of occultation observation compiled with colleagues' observations, whose observer is identified by the number noted outside of each figure*. The thick lines are the author's observation, and the thin lines are of colleagues. The number at the upper right of each figure corresponds to occultation number in Table 1. The dot lines are the center lines of prediction, and the short dashed ellipses are the results of fitting of asteroid dimensions.

* (1) Tomioka, H., (2) Uchiyama, Sh., (3) Yamamura, H., (4) Kitazaki, K., (5) Hirose, T., (6) Ida, M., (7) Ishida, M., (8) Asai, A., (9) Watanabe, Hi., (10) Watanabe, Ha., (11) Ikari, Y., (12) Owada, M., (13) Yoshihara, H., (14) Hosoi, K., (15) Fukui, K., (16) Isobe, K., (17) Hatanaka, A., (18) Akitaya, H., (19) Takimoto, M., (20) Kasebe, H., (21) Yamashita, Y., (22) Uno, M., (23) Mizutani, M., (24) Nemoto, T., (25) Hashimoto, G., (26) Horikawa, T.

each of which is achieved with colleagues whose names are given in figure caption. The thick lines are the author's observation, and the thin lines are of colleagues. Many of colleagues are amateur observers and the members of IOTA/EA.

Fig. 3a shows occultation #5 by the asteroid (702)Alauda, whose shape can be figured out by the 13 observations. Fig. 3b shows occultation #19 by the asteroid (223)Rosa, whose northern boundary is clearly indicated by the author's observation. Fig. 3c

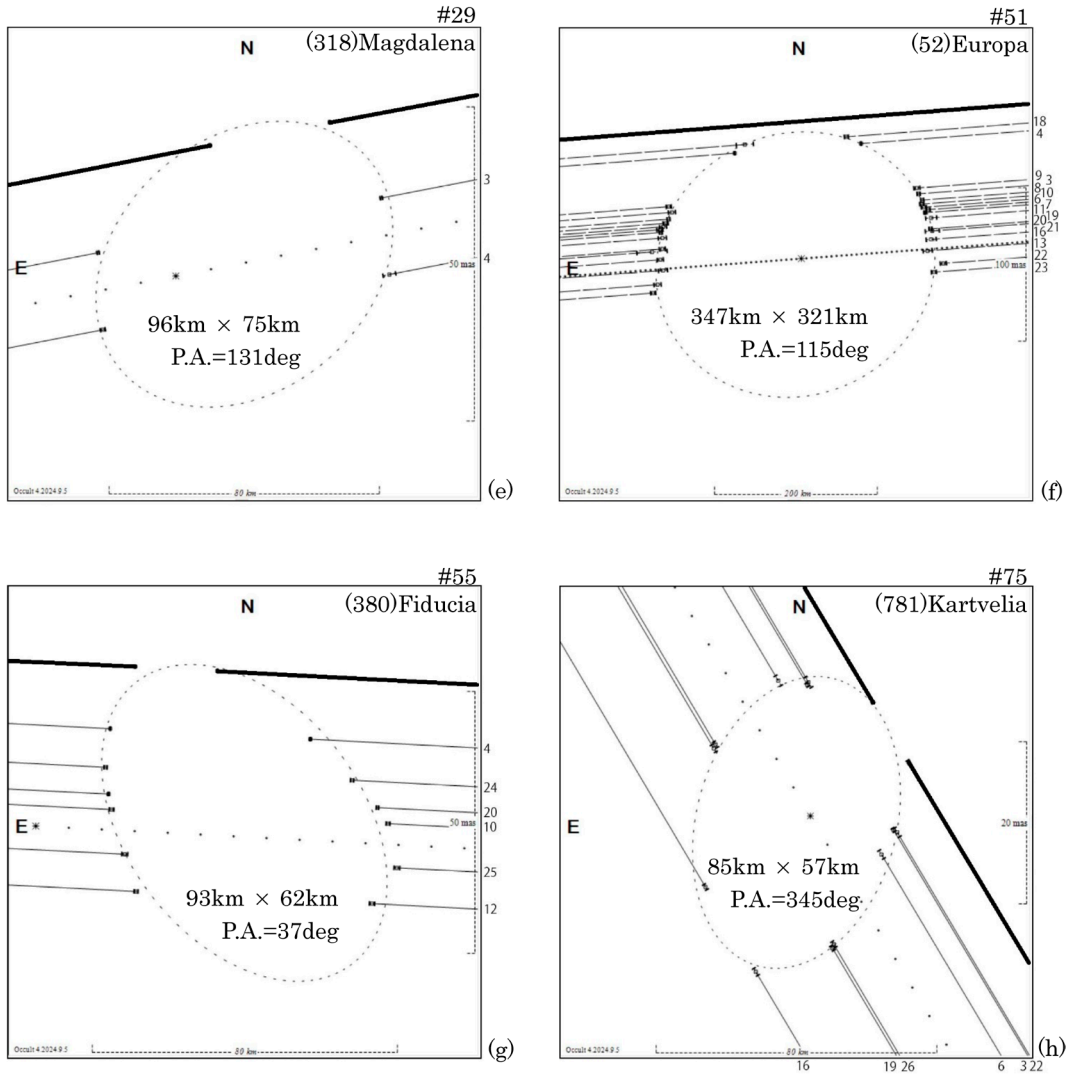


Fig. 3. (Continued)

of occultation #20 by the asteroid (336)Laciedera, whose shape seems a little irregular on the southern side, is another example in which its southern boundary is in sight by the author's observation. The duration of occultation #21 by the asteroid (588)Achilles was long at Tsukuba compared with the prediction, and Fig. 3d shows that the shape of the asteroid is elongated to the south. The author's observation of occultation #29 by the asteroid (318)Magdalena contributes to determine its elliptic shape (Fig. 3e). In the occultation #51 by the asteroid (52)Europa that was one of the successful observations in which many observers participated, the author observed passage

and restricted the northern limit of the asteroid (Fig. 3f). In the occultation #55 by the asteroid (380)Fiducia, another example catching northern boundary of the asteroid (Fig. 3g) as well as #75 by (781)Kartvelia (Fig. 3h), the occultation occurred several seconds earlier than expected, and the observation contributed to the astrometry, i.e., refinement of the orbital element of the asteroid and of the position of the target star. The data of occultation #11 by the Centaur-type asteroid (60558)Echeclus, which also shows cometary activity, was investigated not only for the main body but also for the surroundings such as rings, and the detailed results are described in Pereira *et al.* (2024)⁽¹⁰⁾.

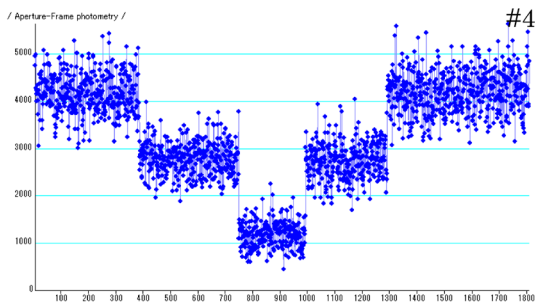


Fig. 4. Light curve of the occultation #4 by the asteroid (451)Patientia, in which the brightness clearly decreases and increases two times.

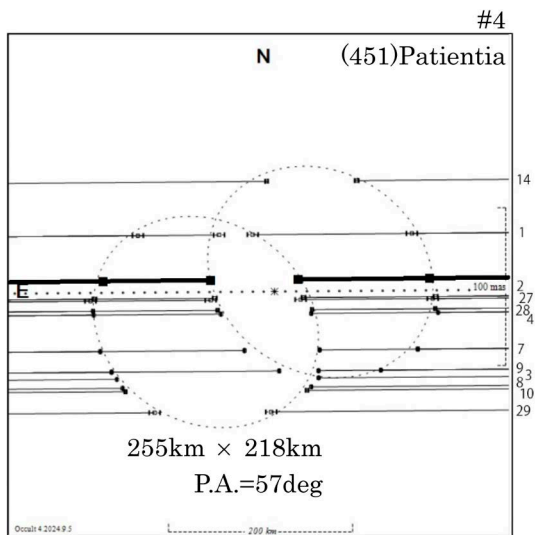


Fig. 5. Results of occultation #4 compiled with colleagues' observations showing that the target star is a close double star whose separation is 0.0794 arcsec. The thick lines are the author's observation, and the thin lines are colleagues', which are identified by the same numbers as Fig. 3. The number 27 is of Nakamura, K., 28 is Sasanuma, N., and 29 is Nakamura, Y.

Fig. 4 is the interesting light curve of occultation #4 by the asteroid (451)Patientia which is described in Table 2 as 1st drop and 2nd drop. The cause of the drops is interpreted due to a close double star whose separation and position angle is 0.0794 arcsec and 113.9 degree respectively as shown in Fig. 5. This is an example of detecting double star by asteroidal occultation.

4. Summary

The author introduced frame-integrating video camera, and began observation in 2019. In these five and a half years, 76 occultations have been observed by this new camera, which significantly increases the opportunities of observing faint phenomena, 14 times/year, while the observation by previous non-integrating camera was 4 times/year. The limiting magnitude of occulted star has fallen to 15th magnitude from 12th magnitude, and the frequency of detecting magnitude drop has increased to 7 times/year. The observations are compiled with colleagues' to get information such as on the shapes and orbital elements. IOTA/EA, which was established last year, is expected to promote occultation research in East Asia.

Acknowledgements

The author would first like to express respect to colleagues, many of whom are amateur observers. The author thanks as well to Mr. David Herald, who develops the indispensable tool for observation, Occult, and also to Mr. Kazuhisa Miyashita, who develops the excellent tool for data analysis, Limovie.

References

- Horaguchi, T., 2018. Observation of Asteroidal Occultation with Time-inserted Video Recording System. *Bull. Natl. Mus. Nat. Sci., Ser. E*, 41: 1–6.
- Hayamizu, T., M. Sōma, H. Geshiro and T. Hashiguchi, 2001. Development of a New Device for Precise Timing. *Report of Natl. Astron. Obs. Of Japan*, 5: 73–79 (in Japanese).
- Hayamizu, T., GHS-OSD information (in Japanese): <http://www2.synapse.ne.jp/haya/ghsod/ghsod.html>
- International Occultation Timing Association (IOTA): <https://occultations.org/>
- IOTA, Resources for Occult: <https://occultations.org/observing/software/occult/>
- Yoshida, F., 2023. Forming a New Occultation Observation Group in East Asia. *Journal for Occultation Astronomy*, 13(4): 27–29.
- IOTA/EA – IOTA East Asia: <https://www.perc.it-chiba.ac.jp/iota-ea/wp/>
- Miyashita, K., T. Hayamizu and M. Sōma, 2006. LIMOVIE,

- a New Light Measurement Tool for Occultation Observation Using Video Recorded. *Report of Natl. Astron. Obs. Of Japan*, 9: 1–26 (in Japanese).
- 9) Miyashita, K., Light measurement tool Limovie: https://astro-limovie.info/limovie/limovie_en.html
- 10) Pereira C. L., F. Braga-Ribas, B. Sicardy, A. R. Gomes-Júnior, J. L. Ortiz, H. C. Branco, J. I. B. Camargo, B. E. Morgado, R. Vieira-Martins, M. Assafin, G. Benedetti-Rossi, J. Desmars, M. Emilio, R. Morales, F. L. Rommel, T. Hayamizu, T. Gondou, E. Jehin, R. A. Artola, A. Asai, C. Colazo, E. Ducrot, R. Duffard, J. Fabrega, E. Fernandez-Valenzuela, M. Gillon, T. Horaguchi, M. Ida, K. Kitazaki, L. A. Mammata, A. Maury, M. Melita, N. Morales, C. Moya-Sierralta, M. Owada, J. Pollock, J. L. Sanchez, P. Santos-Sanz, N. Sasanuma, D. Sebastian, A. Triaud, S. Uchiyama, L. Vanzi, H. Watanabe and H. Yamamura, 2024. Physical properties of Centaur (60558) 174P/Echeclus from stellar occultations. *Monthly Notices of Royal Astron. Society*, 527: 3624–3638.